Climatic Change (2013) 119:435–449
DOI 10.1007/s10584-013-0722-7

Phenology shift from 1989 to 2008 on the Tibetan Plateau: an analysis with a process-based soil physical model and remote sensing data

Zhenong Jin · Qianlai Zhuang · Jin-Sheng He · Tianxiang Luo · Yue Shi

Received: 17 September 2012 / Accepted: 13 February 2013 / Published online: 19 March 2013

Abstract Phenology is critical to ecosystem carbon quantification, and yet has not been well modeled considering both aboveground and belowground environmental variables. This is especially true for alpine and pan-arctic regions where soil physical conditions play a significant role in determining the timing of phenology. Here we examine how the spatiotemporal pattern of satellite-derived phenology is related to soil physical conditions simulated with a soil physical model on the Tibetan Plateau for the period 1989–2008. Our results show that spatial patterns and temporal trends of phenology are parallel with the corresponding soil physical conditions for different study periods. On average, 1 °C increase in soil temperature advances the start of growing season (SOS) by 4.6 to 9.9 days among

Electronic supplementary material The online version of this article (doi:10.1007/s10584-013-0722-7) contains supplementary material, which is available to authorized users.

Z. Jin · Q. Zhuang
Department of Earth, Atmospheric and Planetary Sciences, Purdue University, West Lafayette, IN 47907, USA

Z. Jin (✉)
Ecological Sciences and Engineering, Interdisciplinary Graduate Program, Purdue University, West Lafayette, IN 47907, USA
e-mail: jin77@purdue.edu

Q. Zhuang
Department of Agronomy, Purdue University, West Lafayette, IN 47907, USA

J.-S. He · Y. Shi
Department of Ecology, College of Urban and Environmental Science, Peking University, Beijing 100871, China

J.-S. He
Key Laboratory of Adaptation and Evolution of Plateau Biota, Northwest Institute of Plateau Biology, Chinese Academy of Sciences, Xining 810008, China

T. Luo
Key Laboratory of Tibetan Environment Changes and Land Surface Processes, Institute of Tibetan Plateau Research, Chinese Academy of Science, Beijing 100085, China

different vegetation types, and postpones the end of growing season (EOS) by 7.3 to 10.5 days. Soil wetting meditates such trends, especially in areas where warming effect is significant. Soil thermal thresholds for SOS and EOS, defined as the daily mean soil temperatures corresponding to the phenological metrics, are spatially clustered, and are closely correlated with mean seasonal temperatures in Spring and Autumn, respectively. This study highlights the importance and feasibility of incorporating spatially explicit soil temperature and moisture information, instead of air temperature and precipitation, into phenology models so as to improve carbon modeling. The method proposed and empirical relations established between phenology and soil physical conditions for Alpine ecosystems on the Tibetan plateau could also be applicable for other cold regions.

1 Introduction

Phenology, by definition, means the timing of recurring biological phases (e.g. unfolding of leaves) (Menzel et al. 2006; Linderholm 2006). As a consequence of global climate warming and changes in precipitation regime (Hansen et al. 2010; IPCC 2007), substantial fluctuations in the onset and dormancy of vegetation growth have been widely detected in the last century (Linderholm 2006). Altered phenology will in turn feedback to climate through changing biogeochemical cycling and biophysical properties (e.g. albedo) (Penuelas et al. 2009). Improved understanding of annual rhythm of phenology is therefore critical to having reliable terrestrial biosphere models and climate models (Richardson et al. 2012).

Long-term phenological observations from satellites provide good opportunities to study the phenology changes at the global scale (Linderholm 2006). For example, based on Global Inventory Modeling and Mapping Study's (GIMMS) NDVI (normalized Difference Vegetation Index) datasets, Zhou et al. (2001) reported the start of growing season (SOS) advanced on average by 7 days in Eurasia and by 8 days in North America from 1982 to 1999, while a delayed trend of the end of growing season (EOS) is also documented by Jeong et al. 2011. Overall, the growing season length (GSL) is found to have been extended by nearly 2 weeks since the 1980s (Linderholm 2006). However, the trend for increasingly robust vegetation growth seems to be stalled or even shifted in the recent decade over the Northern Hemisphere (Jeong et al. 2011; Piao et al. 2011b), possibly due to the cooling of regional spring temperature (Piao et al. 2011a; Zhang et al. 2004), winter warming induced later fulfillments of chilling requirements (Korner and Basler 2010), and drought (Zhao and Running 2010).

The Tibetan Plateau, known as "the Roof of the World", is an ideal region to study the response of natural ecosystems to climatic changes due to its unique climate and less human disturbances (Zhuang et al. 2010). Further, previous studies have shown that this region is undergoing severe climate change with a warming and drying trend (Xie et al. 2010; Yang et al. 2010). Major ecosystems on the Tibetan Plateau include desert, alpine grassland and temperate forest, and together act as a small carbon sink (Zhuang et al. 2010). However, the strength of the carbon sink may change due to future warming since the ecosystems on the plateau are highly sensitive to climate changes (Piao et al. 2011a; Zhuang et al. 2010). Phenology is critically linked to photosynthesis, therefore will greatly affect the carbon sink and source activities on the Tibetan Plateau (Shen et al. 2011).

Major environment factors controlling phenology include temperature (Körner 2007), water availability (Jeong et al. 2011; Shen et al. 2011), and photoperiod (Körner 2007; Körner and Basler 2010). However, the dominant factors at the global scale vary with locations (Jolly et al. 2005). In alpine and arctic regions, temperature is the most important

limiting factor that controls the timing of phenology (Körner 2007; Zhang et al. 2004). Quite a few studies show that seasonal temperature controls vegetation phenology shift on the Tibetan Plateau (Piao et al. 2011a; Shen et al. 2011; Yu et al. 2010). Water availability is also considered an influential factor (Jolly et al. 2005; Zhang et al. 2004). However, the magnitude and sign of the effects on the Tibetan Plateau are controversial (Piao et al. 2011a; Shen et al. 2011).

Although much effort has been made in the above mentioned studies to characterize the phenology shift and its association with climate change, there are still apparent knowledge gaps. First, meteorological data from the sparsely distributed meteorological stations adopted in previous studies are insufficient to well represent the regional conditions (Piao et al. 2011a), and are at high risks of human disturbance, given that most of these stations are located in urban areas. Second, soil temperature rather than air temperature should be used when studying the phenology, since it is a more direct control on the vegetation growth due to the prevalent freezing-thawing process of soil in alpine and arctic regions. Third, precipitation alone is questionable as a substitution of water availability under thawing permafrost conditions (Yang et al. 2010) and enhanced evapotranspiration (Xie et al. 2010).

The goal of this study, with a spatial domain of the Tibetan Plateau and temporal span of 1989–2008, is to provide a better method for modeling phenology in cold regions. We first derived the phenology information from satellite data. Second, we simulated soil temperature and moisture dynamics with a process-based ecosystem model, the Terrestrial Ecosystem Model (TEM) (Zhuang et al. 2004), which has been verified to reasonably reproduce the dynamics of field observations of soil temperature and moisture with different time steps and various spatial resolutions (Zhuang et al. 2001, 2002; Tang and Zhuang 2011). Third, we characterized the localized effect of soil temperature and moisture change on phenology shift. Finally, the spatiotemporal patterns of soil thermal thresholds, defined as daily mean soil temperature corresponding to SOS and EOS, were evaluated.

2 Methods

2.1 Model description

The TEM is a global-scale ecosystem model, originally designed to make monthly estimations of carbon and nitrogen fluxes and pool sizes of the terrestrial biosphere, by using spatially referenced information on climate, topography, soils and vegetation (Zhuang et al. 2010). Within TEM, two sub-models, namely the soil thermal model (STM) and the updated hydrological model (HM), are coupled to provide daily soil temperature and soil water content simulation, respectively.

The STM is an extended version of the Goodrich model (Goodrich 1978) with the capability to operate with either 0.5-h or 0.5-day internal time steps and to be driven by either daily or monthly air temperature (Zhuang et al. 2001). The vertical profile in the STM is divided into 6 layers, including snow cover, moss, upper organic soil, lower organic soil, and upper mineral soil and lower mineral soil layers. Within each layer, there are several sub-layers, whose locations are abstracted as nodes at the middle of each sub-layer sequentially (Online Resource A.1). The dynamics of phase changes in the soils column are also simulated. To run STM, simulation depth steps and layer specific information of layer thickness and thermal properties also need to be prescribed as parameters.

The HM represents a major revision of the Water Balance Model (WBM) (Vorosmarty et al. 1989), and was developed to simulate the hydrological dynamics of the soil profile (Zhuang et al. 2002). The HM considers the dynamics of eight state variables for water, and simulates changes in these state variables and water fluxes at a daily time step (Online Resource A.2). The HM is further revised to include: (1) the consideration of surface runoff when determining infiltration rates, (2) the implementation of the effects of temperature and vapor pressure deficit on canopy water conductance, (3) a more detailed representation of water storage and fluxes within the soil profile of upland soils based on the Richards equation, and (4) the development of daily estimates of soil moistures and water fluxes within the soil profile (Zhuang et al. 2004).

2.2 Model parameterization and verification

Values for some parameters of STM could be found in publications (e.g. Zhuang et al. 2010; Tang and Zhuang 2011), while others were determined by calibration. In this study, we developed localized parameters for six major vegetation types on the Tibetan Plateau (Fig. 1 and Table 1). The climate data to drive the STM were interpolated by inverse distance method with both European Reanalysis (ERA) interim reanalysis data and observations from meteorological stations. Specifically, we added elevation as a covariant when interpolating the air temperature. Soil temperatures at 13 sites (Table 1) used to calibrate the model and verify the parameters were daily means based on field measurements from automatic thermal probes (Hobo U12, Onset Computer Corp., MA, USA) buried at 10cm depth with a time step of 1 h.

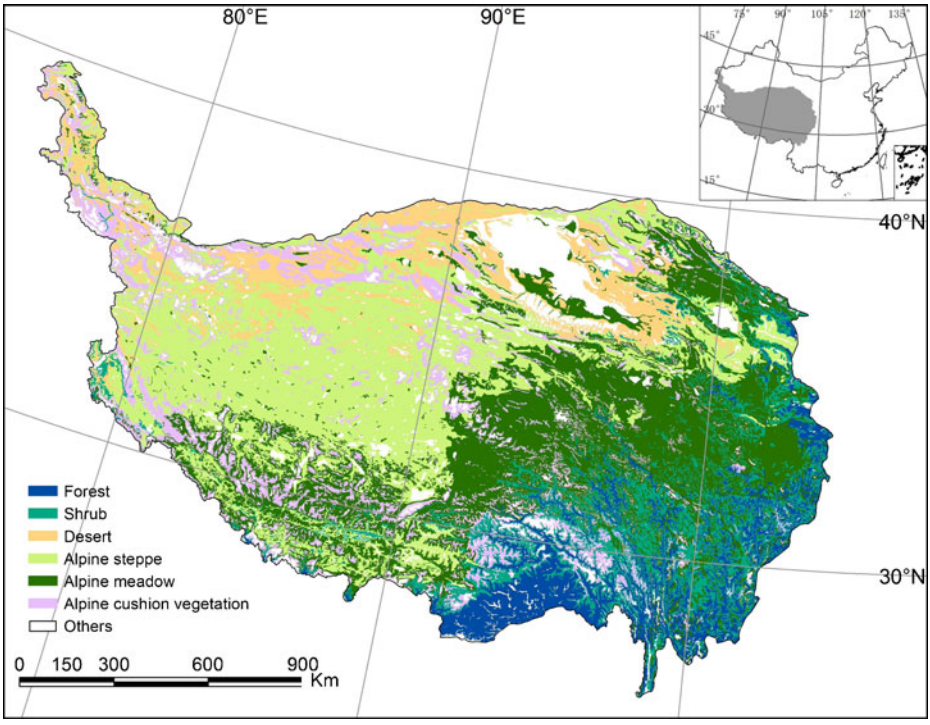

Fig. 1 Vegetation map of the Tibetan Plateau with field sites, redrawn from the Vegetation Map of China

Table 1 Geographic, vegetation and simulation information of calibration (1–6) and verification (7–13) sites

	Site	Longitude (degree)	Latitude (degree)	Elevation (m)	Vegetation type	R^2	RMSE(°C)				
							Overall	Spring	Summer	Autumn	Winter
1	Peak of Mt Sergyemla	94.6	29.6	4320	Forest	0.85	1.52	2.13	2.11	0.78	0.78
2	Laji Mt	101.48	36.37	3454	Shrub	0.94	1.76	1.84	1.82	1.70	1.69
3	Chaka	98.94	36.86	3161	Desert	0.98	1.92	1.97	2.59	1.57	1.54
4	Qumalai	95.8	34.01	4201	Alpine steppe	0.96	1.84	2.07	2.38	1.57	1.39
5	Haibei Station	101.31	37.61	3196	Alpine meadow	0.92	2.40	1.43	3.38	2.57	1.95
6	Peak of Mt Tanggula	91.91	32.88	5244	Alpine cushion	0.90	2.65	2.61	1.93	1.84	3.51
7	Golmud	94.82	36	3312	Desert	0.97	2.06	1.83	2.55	1.57	2.16
8	Guinan	101.08	35.58	3416	Alpine steppe	0.95	2.06	2.91	1.82	1.61	1.79
9	Tuotuo He	92.58	34.32	4556	Alpine steppe	0.94	1.96	2.37	1.76	1.51	2.07
10	Station of Mt Fenghuo	92.89	34.72	4801	Alpine meadow	0.95	2.22	2.12	1.43	1.15	3.16
11	Gande	99.4	34.06	4231	Alpine meadow	0.92	2.20	1.10	1.98	2.92	2.27
12	Naqu	92.02	31.44	4486	Alpine meadow	0.90	2.15	2.15	1.86	2.20	2.29
13	Peak of Mt Kunlun	94.04	35.6	4706	Alpine cushion	0.94	2.73	2.40	3.23	1.76	3.16

The calibration was done by minimizing the distance between observed and simulated soil temperature at each site from January 1st, 2007 to December 31th, 2008. The definitions and values of parameters for each of the six biomes were listed in Online Resource (A.3). Since our primary goal is to simulate the soil temperature at 10 cm depth, we only calibrate parameters for the first two layers while keep the rest as same as prescribed in Zhuang et al. (2010). For HM, we determined the parameter values according to our previous studies in Alaska (Tang and Zhuang 2011) and on the Tibetan Plateau (Zhuang et al. 2010).

2.3 Regional simulation

We applied TEM at a spatial resolution of 8 km×8 km, so as to be consistent with the NDVI dataset. To run TEM on a regional scale, spatially explicit information on climate, topography, vegetation and soils are required. Elevation derived from the Shuttle Radar Topography Mission (SRTM) and soil texture information from the FAO-UNESCO soil map (1971) was organized in our previous study (Zhuang et al. 2010). Vegetation information was derived from 1:1,000,000 vegetation map of China (Chinese Academy of Sciences 2001). The original electronic vector map was first converted to a 1 km×1 km raster version, and then aggregated to an 8 km×8 km spatial resolution according to the majority rule. This process preserves the vegetation information, since vegetation distribution is rather continuous on the Tibetan Plateau. The spatially explicit daily climate data, including cloudiness, precipitation, vapor pressure and air temperature were obtained from the ERA-interim reanalysis data. This data set is the latest global meteorological reanalysis product published by the European Centre for Medium-Range Weather Forecasts (ECMWF) from 1989 to present. We resampled these data from the original 0.75°×0.75° resolution to a 8 km×8 km resolution. Again, elevation was used as a covariant during resampling to reduce the bias caused by the topographic effect according to Frauenfeld et al. (2005).

2.4 NDVI data and phenology extraction

We extracted phenological information including SOS, EOS and GSL based on GIMMS NDVI data. The bi-weekly NDVI data, with a spatial resolution of 8 km×8 km, are derived from the Advanced Very High Resolution Radiometer (AVHRR) instrument onboard the NOAA satellite (Tucker et al. 2005). NDVI values for the regions with snow cover, water body, bare soil and extremely sparse vegetation are smaller than 0.1 (Zhou et al. 2001). Therefore, we only consider pixels with growing season (from April to October) mean NDVI values bigger than 0.1. In addition, we excluded the subtropical area with evergreen forests on the southeastern Tibetan Plateau due to lacking seasonality.

To determine SOS and EOS at each pixel based upon NDVI data, we followed the framework in Piao et al. (2011a). However, instead of using maximum change ratio to determine the NDVI thresholds associated with SOS and EOS, we applied the NDVI ratio method provided in Yu et al. (2010) because the former was more easily affected by extremely low NDVI values caused by snow cover and high cloudiness. The NDVI threshold was calculated with 20-year averaged NDVI seasonal curve for each pixel by

$$\mathrm{NDVI}_{\mathrm{thresholds}} = \mathrm{NDVI}_{\mathrm{min}} + [\mathrm{NDVI}_{\mathrm{max}} - \mathrm{NDVI}_{\mathrm{min}}] \times \mathrm{NDVI}_{\mathrm{ratio}},$$

where $\mathrm{NDVI}_{\mathrm{min}}$ is the average of February and March rather than the minimum of annual curve, so as to reduce the impact of snow or ice cover; $\mathrm{NDVI}_{\mathrm{ratio}}$ is 0.2 for SOS and 0.6 for EOS according to Yu et al. (2010).

2.5 Analysis

We conducted a linear regression for each pixel to detect the trend in phenological metrics, soil thermal and moisture condition for three periods: 1989–1999, 1999–2008, and 1989–2008 as a whole. The year 1999 was selected as a breakpoint because previous studies on the Tibetan Plateau have reported a trend change around this year (Piao et al. 2011a; Yu et al. 2010). We then analyzed the association between soil thermal regime, hydrological dynamics and phenology shifts. To check the effect of soil temperature and moisture change on phenology shift, we did a time-series regression analysis (α=0.1) for both SOS and EOS against mean seasonal soil temperature and soil moisture. The soil thermal threshold for SOS and EOS, defined as 5-days moving average of soil temperature at the corresponding Julian days, is calculated for each pixel, and then regressed against the mean seasonal soil temperature. All the analysis was performed using R statistical software (R Development Core Team 2012).

3 Results and discussion

3.1 Site-level soil thermal dynamics

The localized TEM is able to reproduce the annual dynamics of the observed soil temperature at 10 cm for all six biomes (Online Resource A.4), with R^2 mostly larger than 0.9 and root mean square errors (RMSE) around 2 °C (Table 1). In general, the RMSE in spring and autumn is smaller than that in summer and winter, indicating better reliability of the model during the season we focused on. At site 1 from Peak of Mt. Sergyemla, there was an obvious mismatch in spring and early summer, despite the smallest overall RMSE (1.52 °C). The bias might be due to snowpack effects, because this version of TEM only has a crude treatment of snow process. In addition, at sites 3, 4 and 5, the simulated soil temperatures were lower than observations in summer for both 2007 and 2008, and hence led to a large RMSE (2.59, 2.38, 3.38 °C respectively). These scenarios might be caused by the consistently negative bias between ERA-interim temperature data and the field conditions, despite the efforts we made to reduce the bias in spatial interpolation. We believe the simulation results can be improved if both field measured soil and air temperature data are available. For instance, the smallest seasonal RMSE (0.78 °C) occurs at site 1, at which the model was driven by field-observed air temperature.

3.2 Simulated soil thermal and moisture dynamics

The simulated soil temperatures at 10 cm depth vary spatially during the period 1989–2008 (Fig. 2a, d). Areas that experienced weak (between −0.05 and −0.01 °C/year) and mild (between −0.1 and −0.05 °C/year) cooling in spring occurred in the central and southern parts of the Tibetan Plateau, while warming areas located in the northwestern and the most east edge of the plateau. In autumn, except for a small fraction of area (11 %) along northern and eastern edge showing a weak warming trend, over 60 % of the plateau is cooling over the 20 years. The overall spatial pattern of soil temperature trend is comparable with the 20-year air temperature trend based on ERA-interim reanalysis product (Online Resource A.5); only slightly differ in the trend magnitude, possibly due to the buffer of vegetation. The overall cooling trend, however, contradicts some other studies based on air temperature from meteorological station (Xie et al. 2010) or reanalysis data (Frauenfeld et al. 2005). Such a paradoxical conclusion can be explained by dividing the 20-year period into the first decade (1989 to 1999) and second one (1999 to 2008). Soil temperature at 10 cm depth in these two decades is distinctly different. During the first

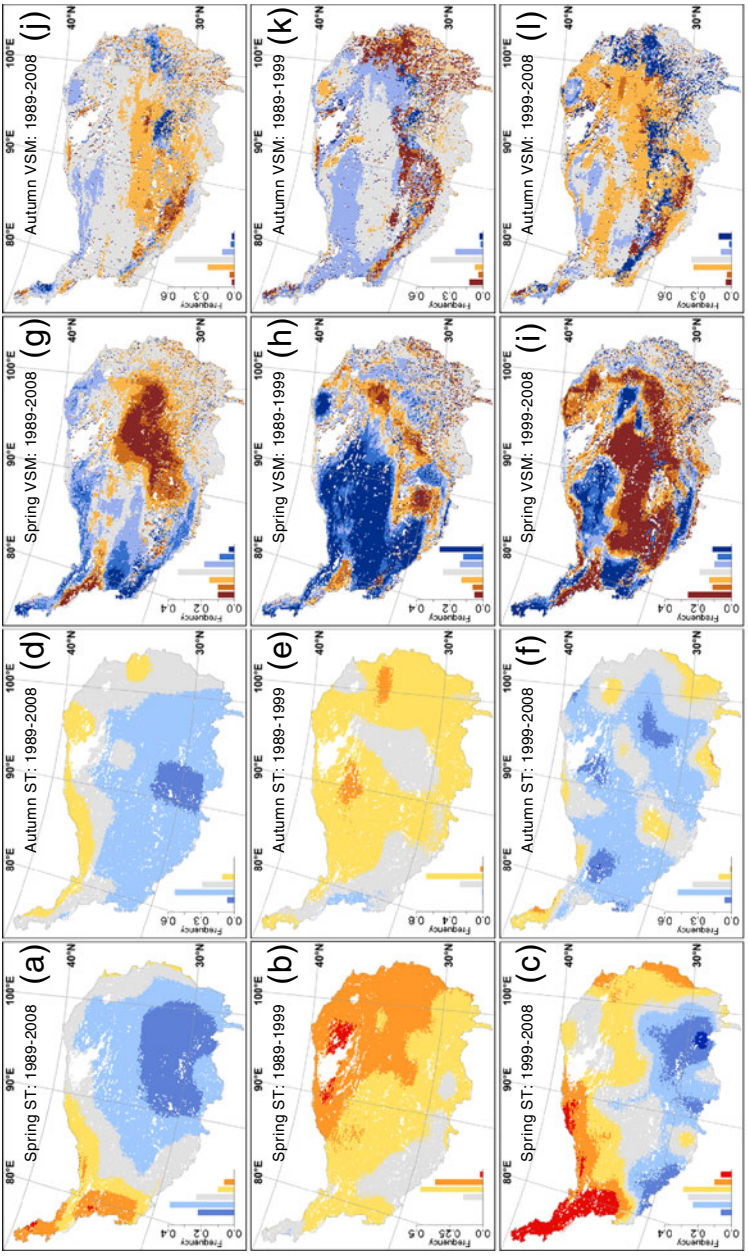

Fig. 2 Spatial patterns of temporal trends in the simulated mean seasonal soil temperature (ST) and volumetric soil moisture (VSM) in both Spring and Autumn during different periods: Spring ST trends during the periods (**a**) 1989–2008, **b** 1989–1999 and (**c**) 1999–2008; Autumn ST trend during (**d**) 1989–2008, **e** 1989–1999 and (**f**) 1999–2008; Spring VSM trends during the periods (**g**) 1989–2008, **h** 1989–1999 and (**i**) 1999–2008; Autumn VSM trends during (**j**) 1989–2008, **k** 1989–1999 and (**l**) 1999–2008. The insets show the frequency distribution of the corresponding trends

decade, 85 % of the plateau in Spring and 71 % in Autumn show a warming trend (Fig. 2b, e), while in the second decade, southern area in Spring and almost all the plateau (88 %) in Autumn have a negative or neutral trend (Fig. 2c, f). Again, the separated soil temperature trend can match air temperature trend spatially in Spring, with only small difference in magnitude. In Autumn, the soil and air temperature trend seems to diverge, possibly due to the aboveground litter in Autumn could act as a heat insulation for soil, which does not exist in Spring. The reversed warming trend in recent years might be a consequence of the increased albedo due to vegetation degradation on the Tibetan Plateau (Chen et al. 2011).

The temporal trend of simulated soil moisture is more heterogeneous spatially than that of soil temperature. From 1989 to 2008, central areas in Spring show a severe drying trend (Fig. 2g), while most of the western part of the Tibetan Plateau seems to become wetter. In Autumn, the drying areas extend towards southwestern, while very limited areas show a positive trend (Fig. 2j). Identically, a distinct spatial pattern can be found in the first and second decades. From 1989 to 1999, there are more wetting areas than drying in both Spring and Autumn (52 % wetting vs. 24 % drying in Spring and 30 % vs. 22 % in Autumn) (Fig. 2h, k). However, from 1999 to 2008, the drying area has doubled in Spring and increased to 43 % in Autumn, mainly occurred in the central and southwestern areas. Our result is comparable with previous study covering similar time span (Xie et al. 2010; Zhuang et al. 2010), but different in regional precipitation trends (Yao et al. 2012). The increasing drying trend in soil moisture can be explained by permafrost degradation in recent years (Yang et al. 2010). The effect of soil water insulation provided by permafrost may weaken substantially with the increased active layer depth and permafrost degradation, which has been widely observed across the Tibetan Plateau (Yang et al. 2010). This also indicates that precipitation alone is not sufficient to represent the changes in soil water availability.

3.3 Spatial pattern of temporal trend of SOS, EOS and GSL

The 20-year averaged SOS, EOS and GSL varied greatly across the Tibetan Plateau (Fig. 3a, b, c). The mean SOS ranges from 105 days (middle April) to 177 days (late June), with an earlier onset in the eastern edge and delayed gradually towards northwestern. Such spatial pattern is consistent with the findings of Yu et al. (2010) and Piao et al. (2011a), and is well explained with the southeast-northwest heat and water gradient. The EOS can be as early as 238 days (late August) in some northeastern parts and be late as 288 days (middle October) in most of the south areas. Compared with SOS, there seems to be a latitudinal effect on EOS, which reflects the photoperiod effect on vegetation senescence (Körner and Basler 2010). Taken together, GSL also shows a southeast to northwest decreasing trend from as high as 178 days to as low as 86 days, and is in agreement with our field observations.

The temporal trends of SOS, EOS and GSL vary spatially for the period 1989–2008 (Fig. 3d, e, f). There are more areas delayed (63 % of total pixels) in SOS than advanced (24 %), with the strongest positive trend (>1 days/year) observed in the central parts. Such spatial pattern is parallel with the 20-year cooling and drying trends of soil physical conditions in Spring. Similarly, EOS advanced in the central and southwestern parts, while delayed in most of the southeastern parts. Overall, the net effect on GSL is shortening in the central and southwestern parts while lengthening in east and southeastern areas (Fig. 3f), which is comparable with the findings of Yu et al. (2010).

Consistent with the trend change in soil temperature and moisture on the Tibetan Plateau, phenology trends also differed substantially between the first decade and the second one (Fig. 3). From 1989 to 1999, SOS advanced over 72 % of the total study region. Such a significant advancing trend is analogous to previous studies covering a similar time span (Piao

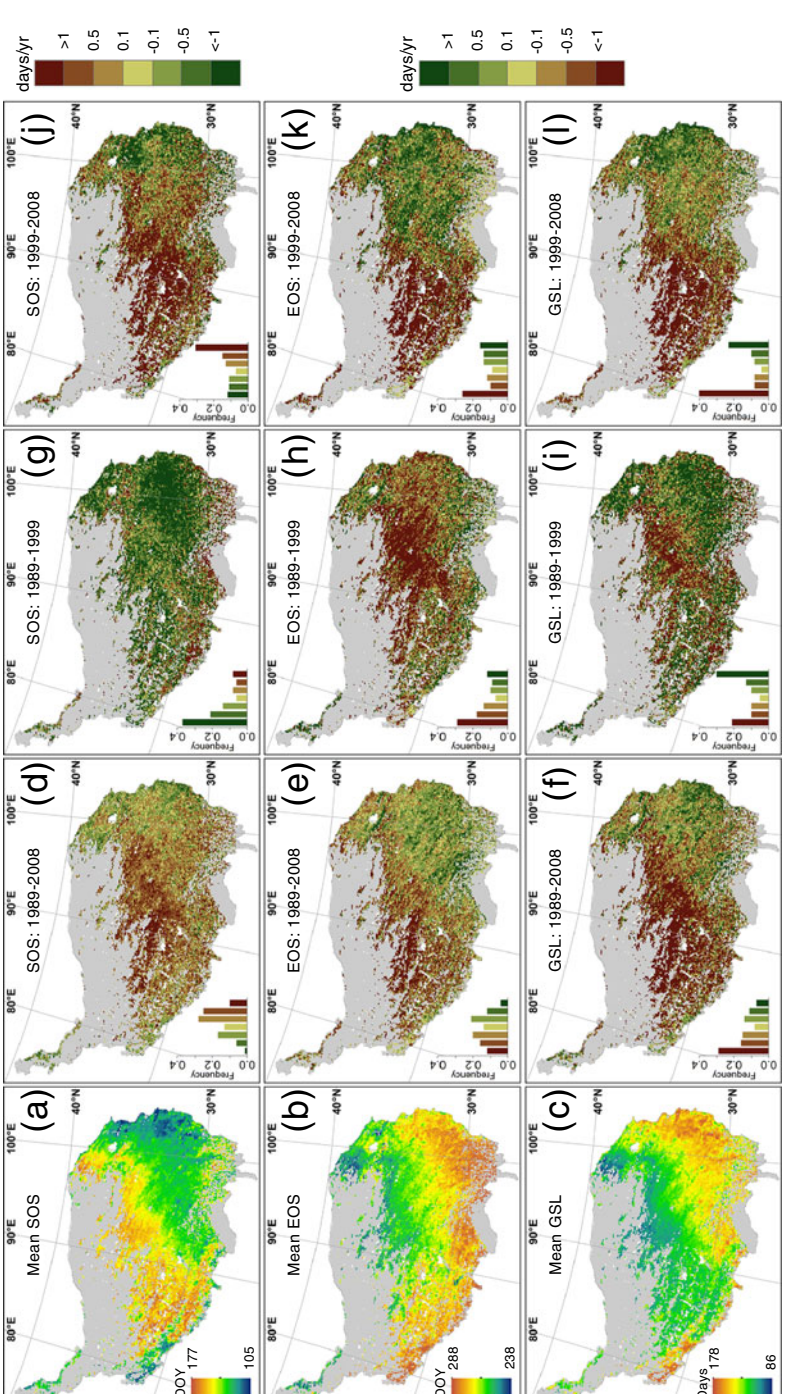

Fig. 3 Spatial patterns and temporal trends in satellite-derived start of growing season (SOS), end of growing season (EOS) and growing season length (GSL) during different periods 20-year averaged (**a**) SOS, **b** EOS and (**c**) GSL for the period 1989–2008; trends in (**d**) SOS, **e** EOS and (**f**) GSL for the period 1989–2008; trends in (**g**) SOS, (**h**) EOS and (**i**) GSL for the period 1989–1999; trends in (**j**) SOS, **k** EOS and (**l**) GSL for the period 1999–2008. *Green color* refers to lengthening effects on GSL, while *brown color* indicates shrinking. The insets show the frequency distributions of the corresponding trends

et al. 2011b; Yu et al. 2010), and can be attributed to the whole plateau warming (Fig. 2b). The locally delayed SOS observed in the south edge of the Tibetan Plateau may result from the Spring drying trend in that area (Fig. 3g). However, with only limited area in the eastern parts showing SOS advancing, the trend of earlier onset of growing season reversed for the period 1999–2008. Around 60 % of the total study region has delayed in SOS (Fig. 3j), with 31 % show a strong trend larger than 1 day/year. The result is similar to the findings of Piao et al. (2011a), who reported a delayed rate of 2.21 days per year from 1999 to 2006 on a regional scale. Considering the extended and increasingly severe drying (Fig. 2i), as well as cooling (Fig. 2c) trend in the central and southwestern parts of the Tibetan Plateau, such a trend change in SOS is reasonable and can be well explained. Trend changes are also obvious for EOS. The extended drying trend towards western parts and wetting trend in eastern area might be possible explanations to the observed westward advancing and eastward delaying trend in EOS after 1999 (Fig. 3k). To sum up, there are more areas showing an increased trend (53 % of total) in GSL than that of a reduced trend during the first decade (Fig. 3i). Meanwhile, in the second decade, almost all the southwestern parts decreased in GSL, while enhanced lengthening of GSL is observed in some eastern parts (Fig. 3l).

The overall shrinking of GSL on the Tibetan Plateau, especially in recent decades, is different from many other studies in China (Piao et al. 2011a; Shen et al. 2011), Europe (Menzel et al. 2006) and North America (Jeong et al. 2011). However, most of the reported lengthened GSL spans to the last century (Linderholm 2006), while increasing evidence from satellite derived NDVI data supports the conclusion of a browning trend of vegetation from this century (Jeong et al. 2011; Piao et al. 2011b). This trend change could be explained largely by the corresponding climate condition, for example, changes in soil temperature and moisture regime as discussed above. At the same time, many other factors like permafrost degradation (Yang et al. 2010) and human activities (Shen et al. 2011) may also influence the phenology dynamics.

3.4 Effect of soil temperature and moisture change on phenology shift

Plants under different ambient climate conditions may have divergent responses to warming and elevated water availability (Sherry et al. 2007). Table 2 listed the effect of 1 unit change of mean seasonal soil temperature and soil moisture on phenology (defined as EST and ESM respectively; positive value means advanced in Julian days while negative value represents delayed). In Spring, 1 °C warming would advance SOS up to 20 days, with most biomes have the mean EST round −9 days/°C. The mean value is higher than the finding (about −3 days/°C for North America and Eurasia) in Zhang et al. (2004) based their analysis on MODIS EVI and LST products. In autumn, the mean EST is between 7.3 days/°C and 10.5 days/°C. Higher absolute values of mean EST

Table 2 Mean effects of 1 °C increase in soil temperature (EST) and 1 % increase in volumetric soil moisture (ESM) on the shift of SOS and EOS. EST and ESM are regression coefficients from time-series analysis. Negative values indicate advancing in Julian days, while positive ones mean delay

	SOS		EOS	
	Mean EST (day/°C)	Mean ESM (day/%)	Mean EST (day/°C)	Mean ESM (day/%)
Forest	−8.2	0.8	8.3	−0.3
Shrub	−8.5	06	7.3	−0.6
Desert	−4.6	−0.1	9.7	−1.7
Alpine steppe	−9.9	1.0	10.5	−0.9
Alpine meadow	−8.7	0.7	9.4	−1.3
Alpine cushion	−9.6	0.7	10.5	−1.1

suggest that vegetation phenology on the Tibetan Plateau is more sensitive to thermal condition change in comparison with other regions.

We also detected a seldom-reported phenomenon that EST and ESM are negatively correlated for most vegetation types in both Spring and Autumn (Fig. 4 and Online Resource A.6). Most of the Pearson correlation coefficients are small between 0.3 and 0.4, and hence any conclusion should be drawn with caution. However, the negatively correlated patterns are true given those small p-values. The negative correlations suggest that, for areas where 1 °C increase in soil temperature lead to more days advance in SOS or EOS, the effect of 1 % increase in soil moisture would go in the opposite direction, i.e. less advance or even delayed in phenology. There seems to be a counterbalance between plant's response to a warmer and wetter environment. More interestingly, the vegetation specific regression line of ESM against EST almost overlaps with each other (Fig. 4 and Online Resource A.6), especially in Spring. These findings, although, are not robust at this moment, may be potentially helpful to clarify the complexity of the climate-driven phenology change. The mechanism behind this phenomenon, however, needs to be further investigated. We conceive that one possible explanation is that elevated soil moisture in areas with larger absolute value of EST (usually colder) will extend the freezing-thawing process of permafrost, and finally drive the phenology to the opposite direction.

3.5 Soil thermal threshold for SOS and EOS

The spatially differed soil thermal thresholds for SOS and EOS (Fig. 5a, b) indicate that no universal definition of thermal threshold can be found. On the other hand, thermal thresholds are somehow spatially clustered. They gradually decrease from the southeast to the north and

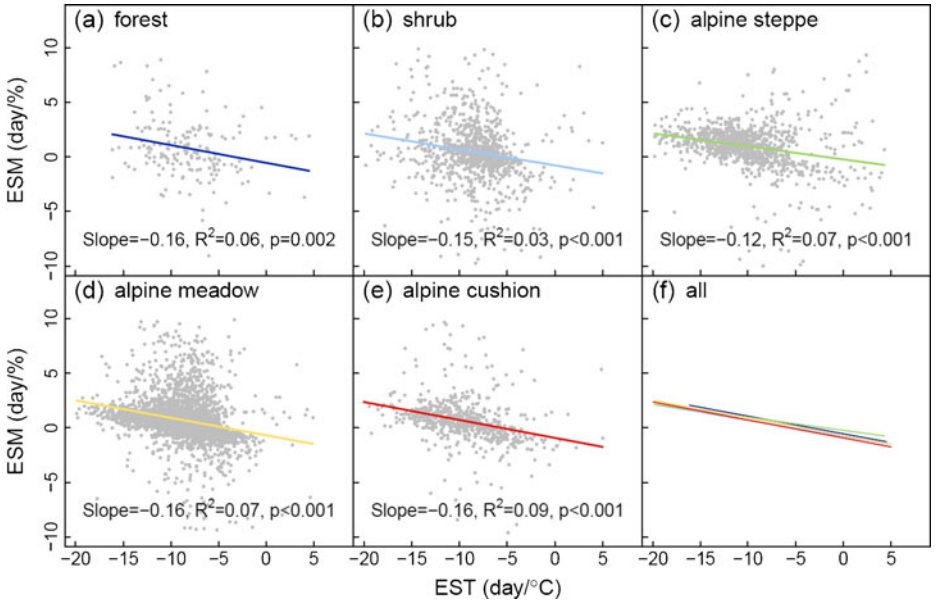

Fig. 4 Vegetation specific relationships between the effect of 1 °C increase in soil temperature (EST) and the effect of 1 % increase in volumetric soil moisture (ESM) on SOS shifts for (**a**) forest, **b** Shrub, **c** alpine steppe, **d** alpine meadow, **e** alpine cushion and (**f**) all. In each panel, the corresponding Pearson correlation coefficient and p-value is listed

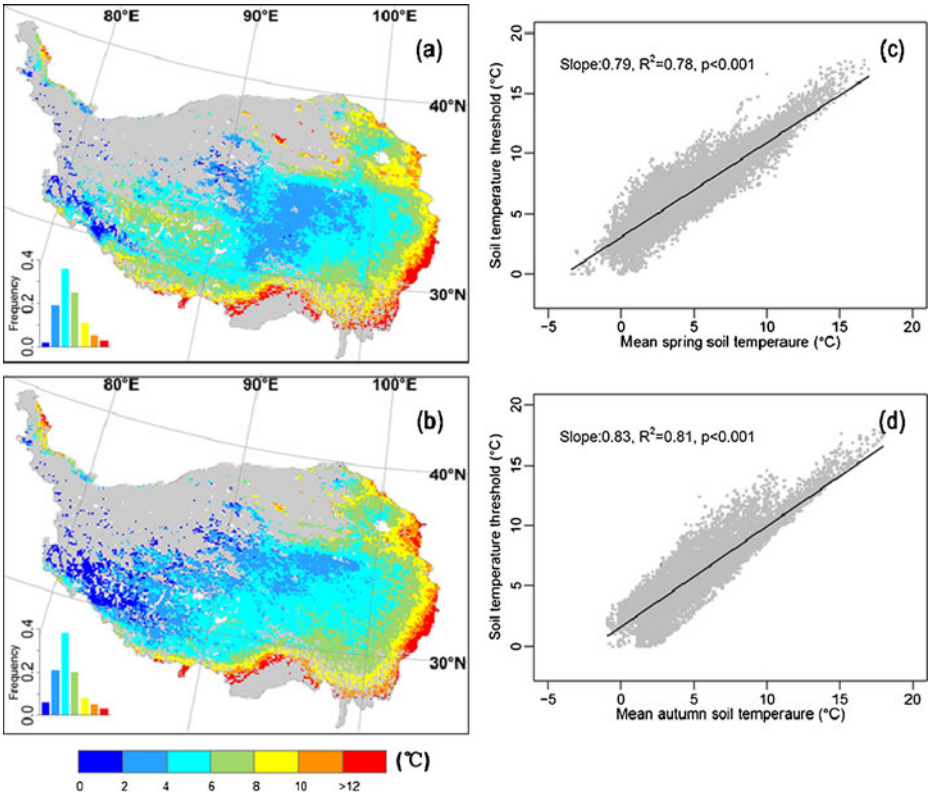

Fig. 5 Spatial patterns of soil thermal thresholds for (**a**) SOS and (**b**) EOS, with the insets showing the frequency distributions of corresponding category, and linear relationships between soil temperature thresholds and mean seasonal soil temperature of (**c**) SOS and (**d**) EOS

the west. The majority area (80 % for SOS and 79 % for EOS) has a threshold between 2 and 8 °C, within the range of thresholds used by many other studies (Körner 2007; Shen et al. 2011). Thresholds lower than 2 °C appear in very limited areas (2 % for SOS and 6 % for EOS), and can be attributed to errors resulted from both NDVI derived phenology date and simulated soil temperatures. In general, no plant growth activity happens between 0 and 2 °C, irrespective of their tolerance to cold environment (Körner 2007).

Linear regressions show that the soil thermal thresholds for both SOS and EOS are significantly and positively correlated with mean seasonal soil temperature when all pixels were included (Fig. 5c, d), which indicates vegetation in a warmer environment requires a higher threshold temperature to start growth and senescence. The linear regression slopes (0.79 for SOS and 0.83 for EOS) are very close to the value (0.76) in Piao et al. (2011a) based on meteorological stations data, suggesting that a 1 °C increase in mean seasonal soil and/or air temperature would lead to about a 0.8 °C increase in thermal threshold for both SOS and EOS. However, this spatial variation law cannot be applied into temporal dimension simply by substituting space for time as proposed by Piao et al. (2011a). We speculate that, the local temperature threshold, as a genetic characteristic (Körner 2007), would keep constant on a decade scale, but has the potential to change on a longer time scale.

Accurate phenology modeling that predicts the start, end, and dynamics of growing season would promise a better understanding of ecosystem productivity and other biogeochemical process, and hence improve the prediction of future climate change. Soil thermal condition is considered as a critical factor controlling the timing and magnitude of vegetation growth in alpine regions (Körner 2007) and pan-arctic ecosystems (Tang and Zhuang 2011; Zhang et al. 2004). Therefore it is a natural step to model phenology as a function of soil temperature and moisture conditions. Moreover, a previous study in New England reported that phenology model with a fixed temperature threshold was not able to capture satellite-derived SOS predictions (Fisher et al. 2007), suggesting that spatially explicit thresholds are required. Taken together, spatially explicit soil thermal thresholds should be incorporated into ecosystem models. These localized soil thermal thresholds are generated through the relations described in Fig. 5.

4 Conclusions and future work

By incorporating satellite-derived NDVI data and model simulated soil physical conditions, this study is the first attempt to link large-scale phenology with two less discussed, but more direct and critical environmental variables in alpine regions, namely, soil temperature and soil moisture, for the period 1989–2008. Our results show that soil temperature and moisture are important predictive factors in determining large-scale phenology. However, weak evidences show that soil wetting will, to some extent, reduce the effect of soil warming on vegetation phenology. Soil temperature thresholds for SOS and EOS are primarily controlled by the long-term local thermal conditions. Our study suggests that soil temperature and moisture information, instead of air temperature and precipitation, should be incorporated into phenology modeling to better quantify carbon budget in alpine cold regions and pan-arctic ecosystems. Next, we will incorporate the empirical relations between soil physical conditions and phenology derived in this study to biogeochemical models (e.g., TEM). We expect the improved phenology will help better quantify carbon dynamics on the Tibetan plateau and other cold regions.

Acknowledgments This research is supported with a NSF project (DEB- #0919331), the NSF Carbon and Water in the Earth Program (NSF-0630319), the NASA Land Use and Land Cover Change program (NASA-NNX09AI26G), Department of Energy (DE-FG02-08ER64599), and the NSF Division of Information & Intelligent Systems (NSF-1028291).

References

Chen H, Zhu QA, Wu N, Wang YF, Peng CH (2011) Delayed spring phenology on the Tibetan Plateau may also be attributable to other factors than winter and spring warming. Proc Natl Acad Sci USA 108:E93–E95

Chinese Academy of Sciences (2001) Vegetation Atlas of China. Science Press, Beijing

Development Core Team R (2012) R: a language and environment for statistical computing. R Foundation for Statistical Computing, Vienna

Fisher JI, Richardson AD, Mustard JF (2007) Phenology model from surface meteorology does not capture satellite-based greenup estimations. Glob Chang Biol 13:707–721

Frauenfeld OW, Zhang TJ, Serreze MC (2005) Climate change and variability using European Centre for Medium-Range Weather Forecasts reanalysis (ERA-40) temperatures on the Tibetan Plateau. J Geophys Res 110:D02101. doi:10.1029/2004JD005230

Goodrich LE (1978) Efficient numerical technique for one-dimensional thermal problems with phase change. Int J Heat Mass Transf 21:615–621

Hansen J, Ruedy R, Sato M, Lo K (2010) Global surface temperature change. Rev Geophys 48:RG4004. doi:10.1029/2010RG000345.1
IPCC (2007) Climate Change 2007: the physical science basis. Cambridge University Press, Cambridge
Jeong SJ, Ho CH, Gim HJ, Brown ME (2011) Phenology shifts at start vs. end of growing season in temperate vegetation over the Northern Hemisphere for the period 1982–2008. Glob Chang Biol 17:2385–2399
Jolly WM, Nemani R, Running SW (2005) A generalized, bioclimatic index to predict foliar phenology in response to climate. Glob Chang Biol 11:619–632
Körner C (2003) Alpine plant life, 2nd edn. Springer, Verlag
Körner C (2007) Significance of temperature in plant life. In: Morison JIL, Morecroft MD (eds) Plant growth and climate change. Blackwell Publishing Ltd, Oxford, pp 48–69
Körner C, Basler D (2010) Phenology under global warming. Science 327:1461–1462
Linderholm HW (2006) Growing season changes in the last century. Agr Forest Meteorol 137:1–14
Menzel A, Sparks TH, Estrella N, Roy DB (2006) Altered geographic and temporal variability in phenology in response to climate change. Global Ecol Biogeogr 15:498–504
Penuelas J, Rutishauser T, Filella I (2009) Phenology feedbacks on climate change. Science 324:887–888
Piao SL, Cui MD, Chen AP, Wang XH, Ciais P, Liu J, Tang YH (2011a) Altitude and temperature dependence of change in the spring vegetation green-up date from 1982 to 2006 in the Qinghai-Xizang Plateau. Agr Forest Meteorol 151:1599–1608
Piao SL, Wang XH, Ciais P, Zhu B, Wang T, Liu J (2011b) Changes in satellite-derived vegetation growth trend in temperate and boreal Eurasia from 1982 to 2006. Glob Chang Biol 17:3228–3239
Richardson AD, Anderson RS, Arain MA et al (2012) Terrestrial biosphere models need better representation of vegetation phenology: results from the North American Carbon Program Site Synthesis. Glob Chang Biol 18:566–584
Shen MG, Tang YH, Chen J, Zhu XL, Zheng YH (2011) Influences of temperature and precipitation before the growing season on spring phenology in grasslands of the central and eastern Qinghai-Tibetan Plateau. Agr Forest Meteorol 151:1711–1722
Sherry RA, Zhou XH, Gu SL et al (2007) Divergence of reproductive phenology under climate warming. Proc Natl Acad Sci USA 104:198–202
Tang J, Zhuang Q (2011) Modeling soil thermal and hydrological dynamics and changes of growing season in Alaskan terrestrial ecosystems. Clim Chang 107:481–510
Tucker CJ, Pinzon JE, Brown ME et al (2005) An extended AVHRR 8-km NDVI dataset compatible with MODIS and SPOT vegetation NDVI data. Int J Remote Sens 26:4485–4498
Vörösmarty CJ, Moore B, Grace AL et al (1989) Continental scale models of water balance and fluvial transport: an application to South America. Global Biogeochem Cy 3:241–265
Xie H, Ye J, Liu X, Chongyi E (2010) Warming and drying trends on the Tibetan Plateau (1971–2005). Theor Appl Climatol 101:241–253
Yang MX, Nelson FE, Shiklomanov NI, Guo DL, Wan GN (2010) Permafrost degradation and its environmental effects on the Tibetan Plateau: a review of recent research. Earth Sci Rev 103:31–44
Yao T, Thompson L, Yang W et al (2012) Different glacier status with atmospheric circulations in Tibetan Plateau and surroundings. Nature Clim Chang. doi:101038/nclimate1580
Yu HY, Luedeling E, Xu JC (2010) Winter and spring warming result in delayed spring phenology on the Tibetan Plateau. Proc Natl Acad Sci USA 107:22151–22156
Zhang XY, Friedl MA, Schaaf CB, Strahler AH (2004) Climate controls on vegetation phenological patterns in northern mid- and high latitudes inferred from MODIS data. Glob Chang Biol 10:1133–1145
Zhao MS, Running SW (2010) Drought-induced reduction in Global Terrestrial Net primary production from 2000 through 2009. Science 329:940–943
Zhou LM, Tucker CJ, Kaufmann RK, Slayback D, Shabanov NV, Myneni RB (2001) Variations in northern vegetation activity inferred from satellite data of vegetation index during 1981 to 1999. J Geophys Res-Atmos 106:20069–20083
Zhuang Q, Romanovsky VE, McGuire AD (2001) Incorporation of a permafrost model into a large-scale ecosystem model: evaluation of temporal and spatial scaling issues in simulating soil thermal dynamics. J Geophys Res-Atmos 106:D24. doi:10.1029/2001JD900151
Zhuang Q, McGuire AD, Mellilo JM et al (2002) Modeling the soil thermal and carbon dynamics of a fire chronosequence in Interior Alaska. J Geophys Res-Atmos 107:8147. doi:10.1029/2001JD001244
Zhuang Q, Melillo JM, Kicklighter DW et al (2004) Methane fluxes between terrestrial ecosystems and the atmosphere at northern high latitudes during the past century: a retrospective analysis with a process-based biogeochemistry model. Global Biogeochem Cycles 18:GB3010. doi:101029/2004GB002239
Zhuang Q, He J, Lu Y, Ji L, Xiao J, Luo T (2010) Carbon dynamics of terrestrial ecosystems on the Tibetan Plateau during the 20th century: an analysis with a process-based biogeochemical model. Global Ecol Biogeogr 19:649–662